8-23-2024

Evaluation of Hi-C Sequencing for Detection of Gene Fusions in Hematologic and Solid Tumor Pediatric Cancer Samples.

Anthony D. Schmitt

Kristin Sikkink

Atif A. Ahmed

Shadi Melnyk

Derek Reid

See next page for additional authors

Recommended Citation

Schmitt AD, Sikkink K, Ahmed AA, et al. Evaluation of Hi-C Sequencing for Detection of Gene Fusions in Hematologic and Solid Tumor Pediatric Cancer Samples. Cancers (Basel). 2024;16(17):2936. Published 2024 Aug 23. doi:10.3390/cancers16172936

cancers

MDPI

Article

Evaluation of Hi-C Sequencing for Detection of Gene Fusions in Hematologic and Solid Tumor Pediatric Cancer Samples

Anthony D. Schmitt [1,*], Kristin Sikkink [1], Atif A. Ahmed [2], Shadi Melnyk [1], Derek Reid [1,†], Logan Van Meter [1,‡], Erin M. Guest [3,4], Lisa A. Lansdon [5,6], Tomi Pastinen [4,5], Irina Pushel [5], Byunggil Yoo [5,6] and Midhat S. Farooqi [4,5,6,*]

1 Arima Genomics, 6354 Corte Del Abeto, Carlsbad, CA 92011, USA; kristin@arimagenomics.com (K.S.); shadi@arimagenomics.com (S.M.); bretreid10@gmail.com (D.R.); vanmeter.logan@gmail.com (L.V.M.)
2 Department of Pathology, Seattle Children's Hospital, Seattle, WA 98105, USA
3 Department of Pediatrics, Division of Hematology & Oncology, Children's Mercy Kansas City, University of Missouri-Kansas City School of Medicine, Kansas City, MO 64108, USA
4 University of Missouri-Kansas City School of Medicine, Kansas City, MO 64108, USA
5 Genomic Medicine Center, Department of Pediatrics, Children's Mercy Kansas City, 2411 Holmes St., Kansas City, MO 64108, USA; ipushel@cmh.edu (I.P.)
6 Department of Pathology & Laboratory Medicine, Children's Mercy Kansas City, University of Missouri-Kansas City School of Medicine, Kansas City, MO 64108, USA
* Correspondence: anthony@arimagenomics.com (A.D.S.); msfarooqi@cmh.edu (M.S.F.); Tel.: +1-617-842-9022 (A.D.S.); +1-816-234-3234 (M.S.F.); Fax: +1-816-302-9944 (M.S.F.)
† D.R. is currently an employee of Neurocrine Biosciences.
‡ L.V.M. is currently an employee of Zafrens.

Simple Summary: Genomic rearrangements are chromosomal abnormalities that alter the arrangement of genes and are important for diagnosing multiple cancer types and guiding therapy selection. However, current diagnostic tests may not detect all genomic rearrangements. Hi-C sequencing is a promising new method for detecting genomic rearrangements. First, we examined whether Hi-C can detect known genomic rearrangements in pediatric leukemia and sarcoma specimens. Next, we evaluated whether Hi-C can detect genomic rearrangements that were not found using standard diagnostic testing. Hi-C showed complete agreement with other diagnostic methods in identifying known rearrangements. Hi-C also detected previously unknown genomic rearrangements in 5/11 pediatric leukemia cases that could impact diagnosis, prognosis, or treatment choices. These data suggest Hi-C could be beneficial for medical diagnostic testing of pediatric cancers, but more extensive clinical validation is needed.

Abstract: Hi-C sequencing is a DNA-based next-generation sequencing method that preserves the 3D genome conformation and has shown promise in detecting genomic rearrangements in translational research studies. To evaluate Hi-C as a potential clinical diagnostic platform, analytical concordance with routine laboratory testing was assessed using primary pediatric leukemia and sarcoma specimens. Archived viable and non-viable frozen leukemic cells and formalin-fixed paraffin-embedded (FFPE) tumor specimens were analyzed. Pediatric acute myeloid leukemia (AML) and alveolar rhabdomyosarcoma (A-RMS) specimens with known genomic rearrangements were subjected to Hi-C to assess analytical concordance. Subsequently, a discovery cohort consisting of AML and acute lymphoblastic leukemia (ALL) cases without known genomic rearrangements based on prior clinical diagnostic testing was evaluated to determine whether Hi-C could detect rearrangements. Using a standard sequencing depth of 50 million raw read-pairs per sample, or approximately 5X raw genomic coverage, we observed 100% concordance between Hi-C and previous clinical cytogenetic and molecular testing. In the discovery cohort, a clinically relevant gene fusion was detected in 45% of leukemia cases (5/11). This study provides an institutional proof of principle evaluation of Hi-C sequencing to medical diagnostic testing as it identified several clinically relevant rearrangements, including those that were missed by current clinical testing workflows.

Keywords: Hi-C sequencing; structural variants; 3D genomics; pediatric oncology

Citation: Schmitt, A.D.; Sikkink, K.; Ahmed, A.A.; Melnyk, S.; Reid, D.; Van Meter, L.; Guest, E.M.; Lansdon, L.A.; Pastinen, T.; Pushel, I.; et al. Evaluation of Hi-C Sequencing for Detection of Gene Fusions in Hematologic and Solid Tumor Pediatric Cancer Samples. *Cancers* **2024**, *16*, 2936. https://doi.org/10.3390/cancers16172936

Academic Editor: Nicola Amodio

Received: 11 July 2024
Revised: 15 August 2024
Accepted: 19 August 2024
Published: 23 August 2024

1. Introduction

Pediatric cancer is the leading cause of disease-induced morbidity and mortality in children in the USA and encompasses a wide range of cancer types, including leukemias, lymphomas, and sarcomas [1]. Advances in sequencing technologies have contributed to a better understanding of the molecular characteristics of these diseases and have provided clues to new markers for targeted therapy [2,3].

While the mutational burden of pediatric cancers is generally lower than their respective adult counterparts [4,5], genomic rearrangements, including gene fusions and other chromosomal rearrangements, are more common drivers in pediatric cancer [3,5,6]. These genomic rearrangements can result in the overexpression or loss-of-function of genes or create entirely new chimeric genes, which may then serve as biomarkers for disease, give information as to prognosis, and/or be therapeutically targetable.

Clinical testing methods for genomic rearrangements are shared across pediatric cancer types including rhabdomyosarcomas and leukemias; commonly used techniques include cytogenetic methods such as karyotyping, fluorescence in situ hybridization (FISH), and chromosomal microarray analysis (CMA). However, analysis of genomic rearrangements in pediatric cancer using these routine cytogenetic testing methods is complicated by several factors. First, live cells must be obtained and grown in culture for karyotyping. This is often not possible for solid tumors where tissue is formalin-fixed and paraffin-embedded (FFPE) and a fresh sample is not set aside for karyotyping analysis, or if karyotyping fails due to poor tumor cell growth in culture [7]. Furthermore, karyotype analysis has a relatively coarse genetic resolution, detecting only structural changes greater than 5–10 Mb, thus rendering some rearrangements cryptic and undetectable [8]. Second, FISH requires the selection of probes for the assay and, therefore, cannot detect genomic rearrangements involving novel genes or, depending on the FISH probe design (breakapart vs. dual fusion), cannot resolve the fusion partner or detect fusions involving novel (unprobed) partners, respectively. FISH also can be fraught with a higher background signal when analyzing FFPE solid tumor tissue, potentiating false negative or false positive calls [9]. Third, CMA is unable to detect balanced genomic rearrangements, which are important known drivers of pediatric cancers [10]. There are also notable strengths of cytogenetic techniques, including relatively fast turnaround time and low limit of detection, as both karyotype and FISH are inherently single-cell resolution techniques. However, these strengths are counterbalanced by operational complexities, which require specialized lab and interpretation expertise to conduct FISH and karyotype analyses, thus limiting the number of clinical laboratories that can perform such analyses [11].

Molecular methods for detecting gene fusions, such as targeted RNA sequencing (RNA-seq) approaches, including anchored multiplex PCR (AMP), are increasingly utilized for detecting gene fusions in solid and hematological cancers [12–15]. However, for solid tumors stored as FFPE samples, RNA degradation can preclude reliable analysis in routine diagnostic use; this issue is further exacerbated for research specimens with longer archival periods [16,17]. Also, even though AMP is partner-agnostic, it still requires the targeting of at least one gene involved in a given gene fusion, thereby missing fusions where both genes are untargeted [15]. More generally, AMP is also insensitive to other types of genomic rearrangements, such as non-coding rearrangements (promoter swaps or enhancer hijacking events) that do not produce fusion transcripts, which are routinely tested for and inform clinical decision-making in hematological cancers, such as acute lymphoblastic leukemia (ALL) [18]. Other molecular methods include optical genome mapping (OGM). Since the benefits of OGM are dependent upon the successful isolation of high molecular weight (HMW) DNA, OGM has been deployed by some clinical labs for hematological cancers where HMW DNA can be isolated and preserved from higher-quality specimens. However, OGM currently cannot be applied to FFPE tissues where the DNA is potentially already fragmented and/or the tissue specimen quality is compromised, thus precluding OGM analyses of FFPE solid tumors [19].

In this study, we evaluated a 3D genomics approach to detect genomic rearrangements in primary pediatric leukemia and sarcoma specimens. The approach, termed Hi-C sequencing, is a DNA-based next-generation sequencing (NGS) method that preserves the 3D conformation of the genome. Hi-C sequencing has emerged as a promising approach for genomic rearrangement detection in translational research studies and has been previously shown to be an accurate and sensitive approach for identifying genomic rearrangements, including inter- and intra-chromosomal translocations and other structural rearrangements [20–30]. However, detailed evaluations of the technology with a focus on analytical concordance relative to routine clinical laboratory testing workflows in solid and hematological cancers are lacking, as is an evaluation of how Hi-C-based testing could impact the diagnostic yield by detecting clinically significant gene fusions, either in the context of supplementing or replacing technologies in current clinical testing workflows. Overall, this study aimed to provide an institutional proof of the principle evaluation of Hi-C for genomic rearrangement detection in pediatric cancer and sought to determine its utility in clinical testing workflows.

2. Materials and Methods

2.1. Overview

First, to evaluate analytical concordance, archived pediatric acute myeloid leukemia (AML) and alveolar rhabdomyosarcoma (A-RMS) specimens with known gene fusions as determined by prior clinical testing were subjected to Arima Genomics' Hi-C sample prep, followed by Illumina sequencing and genomic rearrangement bioinformatics analysis. Next, to explore the potential impact on diagnostic yield using Hi-C, a discovery cohort with additional AML and ALL specimens was analyzed. These specimens had been previously subjected to standard-of-care clinical cytogenetic and/or molecular testing, and no genetic driver/known gene fusion had been identified. Hematologic specimens included frozen white blood cell pellets and viably preserved frozen hematopoietic cells, either from bone marrow aspirates or peripheral blood. For solid tumor specimens, unstained FFPE scrolls were used.

2.2. Samples–Solid Tumors

Pediatric A-RMS specimens were collected by the Children's Mercy Hospital (CMH, Kansas City, MO, USA) as part of the routine diagnostic workflow. Each specimen was formalin-fixed and paraffin-embedded and stored at room temperature. FFPE A-RMS samples (N = 5, archival period range 9–13 years) that were known to be gene fusion-positive as detected by previous clinical testing (i.e., chromosomes, FISH, or microarray) were sectioned to produce unstained tissue scrolls (N = 3 to 5 scrolls per sample) for Hi-C library preparation and sequencing. The average estimated tumor percentage was 86% (range 80–90%). The Hi-C workflow and genetic analyses were performed blinded to the clinical genetic results. A summary of the sample types, preservation methods, archival periods, and estimated tumor percentages are provided in Supplemental Table S1. A retrospective study, including genetic analysis, of de-identified archived paraffin-embedded RMS tissue was approved by the CMH Institutional Review Board (IRB).

2.3. Samples–Leukemias

Leukemia specimens were collected by CMH and put into its biorepository. This was performed in a tumor bank research study approved by the CMH IRB, which included patient consent, as well as collection, processing, and storage of patient samples. Specimens collected prior to 2019 underwent white blood cell (WBC) isolation, were snap-frozen (non-viably), and stored at −80 °C. Specimens collected after 2019 underwent WBC isolation and were gradually frozen (viably) in a preservation media comprising 10% DMSO and tissue culture media and then stored at −80 °C.

For the concordance cohort, five AML specimens were cryopreserved, while two were frozen non-viably (N = 7). Six AML specimens were obtained from bone marrow aspirates,

while one was a peripheral blood specimen (*N* = 7 total; archival period range 1–4 years, Supplemental Table S1). The average estimated blast percentage was 52% (range 11–81%) (Supplemental Table S1). In the concordance cohort, each specimen had undergone clinical standard-of-care cytogenetic (karyotyping, FISH, and/or microarray) and/or molecular testing (targeted cancer NGS sequencing panel, PCR). For five of the specimens, a known gene fusion had been identified. Of these five specimens, the average percentage of cells positive for the gene fusion by prior clinical FISH testing was 79% (range 52–94%) (Supplemental Table S1). For two specimens, no known gene fusions had been identified, and instead, driver alterations other than gene fusions had been detected (e.g., biallelic *CEBPa* mutations). Once again, the Hi-C workflow and genetic analyses were performed blinded to the clinical genetic results.

For the discovery cohort, eight leukemia specimens were cryopreserved, while three specimens were frozen non-viably (*N* = 11). Nine specimens were bone marrow aspirates, and two were peripheral blood specimens (*N* = 11 total), comprising precursor B-ALL, T-ALL, and AML. Archival period ranged from 1–4 years. The average estimated blast percentage was 83% (range 62–98%) (Supplemental Table S1). In the discovery cohort, each specimen had undergone clinical standard-of-care cytogenetic (karyotyping, FISH, microarray) and/or molecular testing (targeted cancer NGS sequencing panel), and no genetic subtype or known gene fusion had been identified. For all leukemia specimens, a summary of the sample types, preservation methods, archival periods, estimated blast percentages, and percentage of cells positive for the gene fusion by prior clinical FISH testing is provided in Supplemental Table S1.

2.4. Arima-HiC Sequencing

For frozen cell pellets or viably-preserved cells isolated from blood, cells were first crosslinked and then subjected to Hi-C sample preparation using the Arima-HiC kit (P/N A51008, Arima Genomics, Carlsbad, CA, USA). For FFPE tissues, 5–10 µm sections were first de-waxed and rehydrated and then subjected to Hi-C sample preparation using the Arima-HiC for FFPE kit (P/N A311038). Subsequently, short-read sequencing libraries were prepared by shearing the proximally ligated DNA, followed by size-selecting DNA fragments using solid phase reversible immobilization (SPRI) beads. DNA fragments containing ligation junctions were then enriched using Enrichment Beads (provided in the Arima-HiC kits) and converted into sequencing libraries using the Swift Accel-NGS 2S Plus kit (Swift Biosciences, Ann Arbor, MI, USA, P/N: 21024). After adapter ligation, DNA was PCR amplified and purified using SPRI beads. The purified DNA underwent standard quality control (qPCR and Bioanalyzer) and was sequenced using a NovaSeq 6000 (Illumina, San Diego, CA, USA) according to the manufacturer's instructions.

2.5. Data Analysis Workflow

Genomic rearrangements were identified using the Arima-SV v1.3 pipeline [31]. The Arima-SV v1.3 pipeline contains several sub-components. First, raw read-pairs are aligned to the human reference genome (hg38) and deduplicated using HiCUP [32]. Genomic rearrangements are called using HiC-Breakfinder, which outputs rearrangement calls where the breakpoints are localized to a genomic bin rather than an individual nucleotide, such as a 1 kb or 10 kb bin [20]. For data visualization, deduplicated alignments from HiCUP are converted into Hi-C matrices using Juicer software (Version 1.19.02) [33], which are then visualized alongside the genomic rearrangement calls using Juicebox [34]. For sub-sampling analyses, raw read-pairs were randomly extracted from the full datasets using a sub-sampling feature of the Arima-SV v1.3 pipeline, and then the sub-sampled raw read-pairs were run through the Arima-SV v1.3 workflow for rearrangement detection and data visualization.

3. Results

3.1. Hi-C Library Preparation and Quality Assessment

Arima-HiC libraries prepared from retrospective leukemia and sarcoma cases were deeply sequenced, and genomic rearrangements were detected using the Arima-SV v1.3 pipeline (Figure 1). Each full sequencing dataset was evaluated for quality using well-established performance metrics for Hi-C data that are output from the Arima-SV v1.3 pipeline (Supplemental Table S2). Of note, within the leukemia specimens, we observed that the data quality for the specimens prepared as frozen non-viable cell pellets was considerably lower than the specimens prepared as frozen viable (cryopreserved) cells. This is most likely due to cells bursting upon non-viable freezing but may also be exacerbated by the archival periods (e.g., 4 years) or other factors. Also of note, the FFPE specimens with an archival period of 9–13 years had relatively low DNA yields and reduced data quality metrics relative to FFPE specimens with shorter archival periods. Lastly, while data quality was assessed using the original full sequencing depths (Supplemental Table S2), we performed all genomic rearrangement analyses in the leukemia and sarcoma specimens at a sub-sampled raw sequencing depth of 50 million raw read-pairs (~5X raw genome coverage). The sub-sampled datasets had quality metrics resembling those of the full-depth datasets except with fewer mapped Hi-C read-pairs available for analysis.

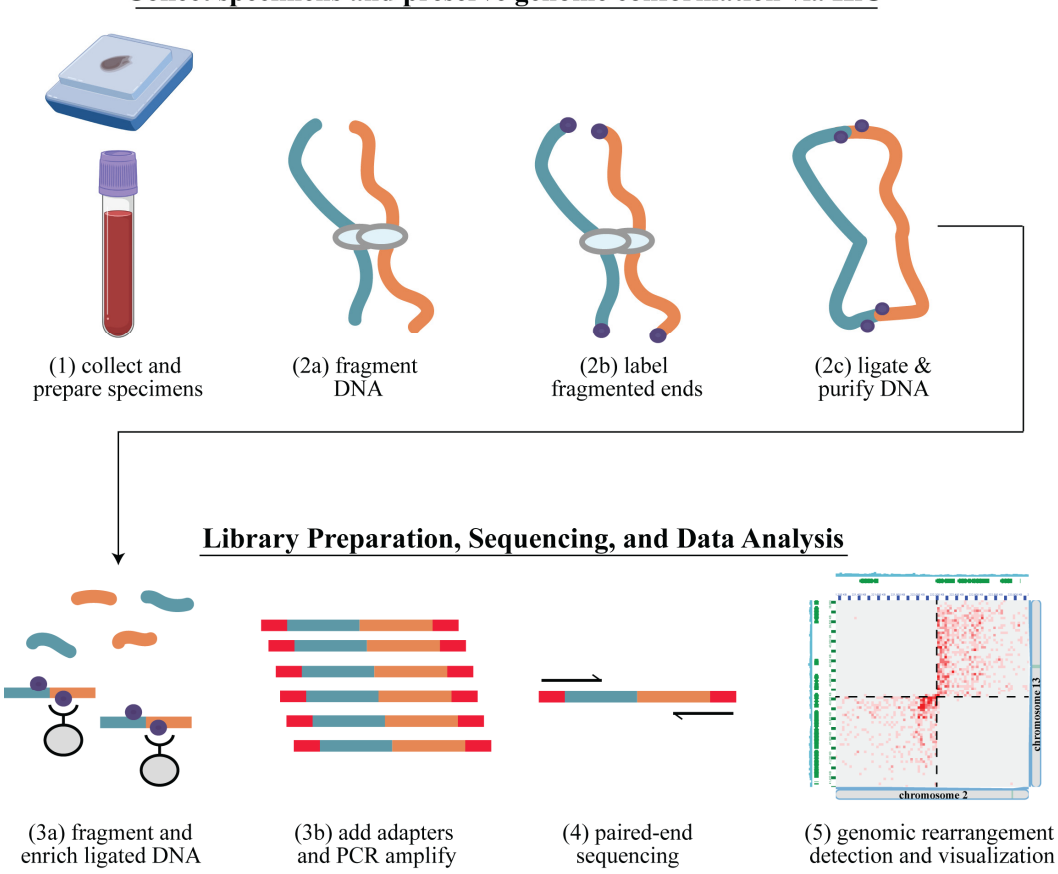

Figure 1. Genomic rearrangement detection using Arima Genomics' Hi-C workflow. (Step 1) collect specimens and prepare for Hi-C testing. For hematologic cancers, extract the white blood cells from the bone marrow aspirates or peripheral blood and crosslink. For formalin-fixed paraffin-embedded (FFPE) solid tumors, de-wax and rehydrate the tissue; (Step 2) preserve the 3D conformation of the genome via Hi-C, resulting in labeled proximity ligated DNA that has preserved 3D conformation information; (Step 3) library preparation, resulting in a sequence-ready Hi-C library; (Step 4) next-generation sequencing (NGS); (Step 5) bioinformatics analysis using the Arima-SV v1.3 workflow to identify genomic rearrangements and visualize results.

3.2. Hi-C Is Concordant with Gold-Standard Methods for Pediatric Cancer Clinical Cytogenetic Testing

We used the sub-sampled datasets to 50 million raw read-pairs to determine concordance with clinical cytogenetic testing. At this depth, the clinically relevant gene fusions in all five previously determined fusion-positive AML cases were detected (two *RUNX1::RUNX1T1* fusions, one *CBFB::MYH11* fusion, one *CBFA2T3::GLIS2* fusion, and one *KMT2A::MLLT4* fusion) (Table 1). For example, in the "AML C6" case, prior clinical testing from karyotype analysis showed an apparent chromosome 11 deletion and translocation with the long arm of chromosome 6. A panel of FISH assays found a *KMT2A* rearrangement with *3′KMT2A* loss, and microarray analysis found deletions of *KMT2A* exons 11–36 and *MLLT4* exon 1 deletion, suggestive of a *KMT2A::MLLT4* fusion. Hi-C analysis detected a genomic rearrangement between chromosome 11 and the long arm of chromosome 6, but also the reciprocal rearrangement when a telomeric portion of chromosome 6 translocated with the long arm of chromosome 11. These findings are apparent when the Hi-C data are viewed at the chromosome scale (Figure 2A), where the "bowtie" signal pattern in the Hi-C data is known to be indicative of a reciprocal inter-chromosomal rearrangement [27]. Upon inspection of the genomic rearrangement breakpoint at higher resolution, the *KMT2A::MLLT4* gene fusion is readily detected, as well as apparent reductions in sequencing coverage at both the 3′ portion of *KMT2A* and the 5′ portion of *MLLT4* (Figure 2B). The Hi-C results were further supported by conventional NGS-based testing (using both DNA and RNA) performed at a commercial reference laboratory, which also detected the *KMT2A::MLLT4* gene fusion.

Table 1. Hi-C is concordant with clinical cytogenetic testing.

Sample ID	Cancer Type	Sample Source	Preservation (If Any)	Prior Cytogenetic Test Result	Hi-C Test Result
AML C1	AML	PBMCs	90% FBS/10% DMSO	*CBFA2T3::GLIS2*	*CBFA2T3::GLIS2*
AML C2	AML	Bone Marrow	None	Negative *	Negative
AML C3	AML	Bone Marrow	None	*RUNX1::RUNX1T1*	*RUNX1::RUNX1T1*
AML C4	AML	Bone Marrow	90% FBS/10% DMSO	*MYH11::CBFB*	*MYH11::CBFB*
AML C5	AML	Bone Marrow	90% FBS/10% DMSO	Negative **	Negative
AML C6	AML	Bone Marrow	90% FBS/10% DMSO	*KMT2A::MLLT4* ***	*KMT2A::MLLT4*
AML C7	AML	Bone Marrow	90% FBS/10% DMSO	*RUNX1::RUNX1T1*	*RUNX1::RUNX1T1*
ARMS C1	A-RMS	Tissue	FFPE	*FOXO1*-r	*PAX3::FOXO1*
ARMS C2	A-RMS	Tissue	FFPE	*PAX3::FOXO1*	*PAX3::FOXO1*
ARMS C3	A-RMS	Tissue	FFPE	*PAX3::FOXO1*	*PAX3::FOXO1*
ARMS C4	A-RMS	Tissue	FFPE	*FOXO1*-r	*PAX7::FOXO1*
ARMS C5	A-RMS	Tissue	FFPE	*FOX7::FOXO1*	*PAX7::FOXO1*

AML = Acute Myeloid Leukemia; A-RMS = Alveolar Rhabdomyosarcoma; PBMC = Peripheral Blood Mononuclear Cell; FBS = Fetal Bovine Serum; DMSO = Dimethyl Sulfoxide; FFPE = Formalin-Fixed Paraffin-Embedded; "-r" indicates when the fusion partner is unknown. * *FLT3* ITD mutation detected (PCR). ** Biallelic *CEBPa* mutations detected (targeted DNA-seq). *** *KMT2A::MLLT4* fusion also detected upon NGS-based fusion testing.

In addition, the clinically relevant gene fusions in all five previously determined fusion-positive A-RMS cases were detected (*PAX3::FOXO1* (*N* = 3) and *PAX7::FOXO1* (*N* = 2)) (Table 1). For example, in the "ARMS C3" case, previous clinical testing from FISH analysis showed evidence for *FOXO1* (FHKR) gene rearrangement and aneuploidy, and karyotype analysis showed t(2;13) indicative of *PAX3::FOXO1* gene fusion. Hi-C analysis detected a reciprocal genomic rearrangement between chromosomes 2 and 13 (Figure 2C), and upon inspection at the genomic rearrangement breakpoint at higher resolution, the *PAX3::FOXO1* gene fusion was readily detected (Figure 2D). Furthermore, because the signal pattern in the Hi-C data is indicative of the type of chromosomal rearrangement, Hi-C analysis can distinguish between chromosomal rearrangements and extrachromosomal rearrangements such as double minutes [35–39]. An analysis of the Hi-C data predicted the chromosomal rearrangement type as double minutes for three of five A-RMS cases and as chromosomal translocations for two of five A-RMS cases. These predictions agreed

with the karyotype analysis for all four cases where karyotype analysis was performed (Supplemental Figure S1).

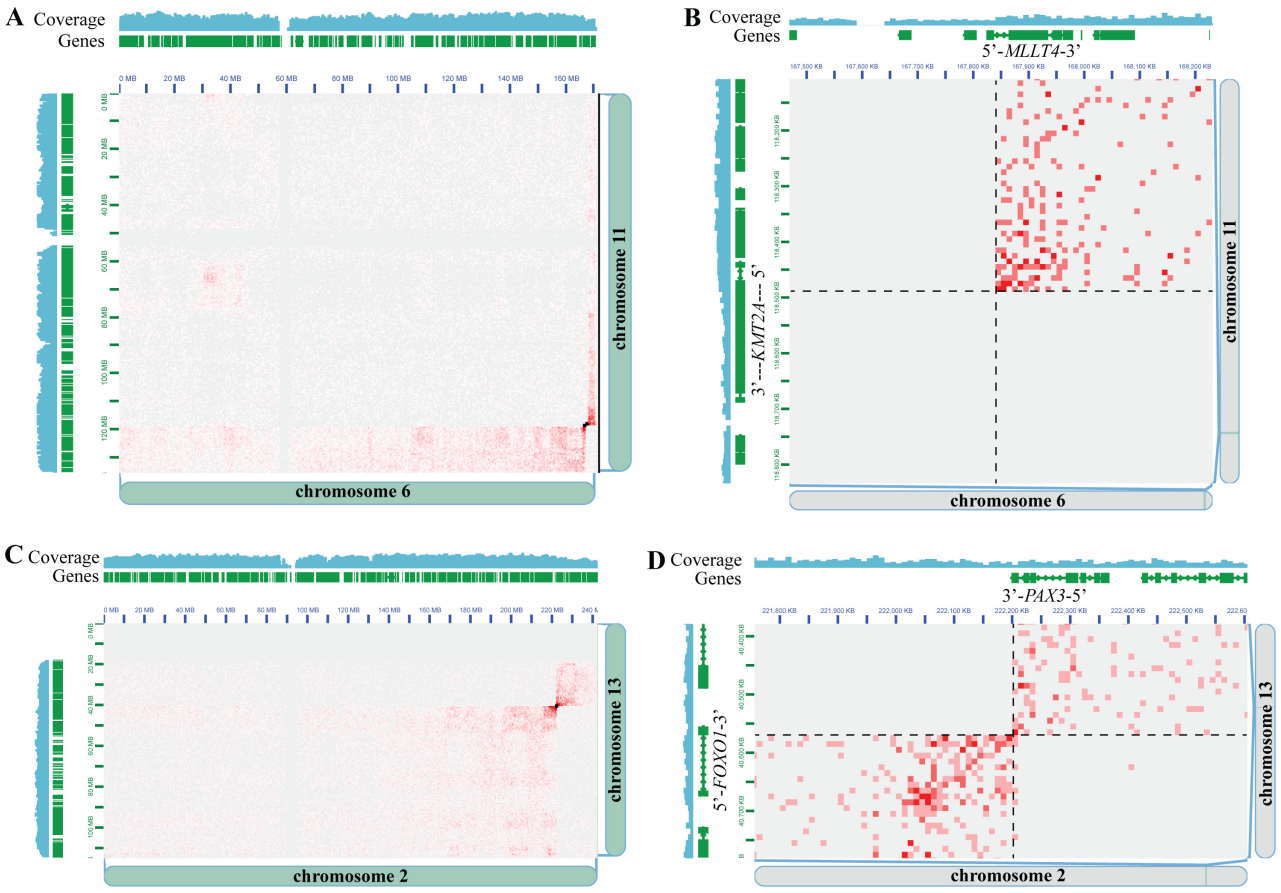

Figure 2. Hi-C is concordant with clinical cytogenetic testing for detecting clinically significant gene fusions. (**A**) Chromosome 6 × Chromosome 11 Hi-C heatmap from specimen "AML C6". Genomic coordinates, gene locations, and sequencing coverage from Chromosome 6 and 11 are shown along the edges of the X and Y axes of the heatmap, respectively. Small black boxes overlaid on the heatmap are the Arima-SV pipeline genomic rearrangement calls. (**B**) Same as panel (**A**), except zoomed-in to the locus around the *KMT2A::MLLT4* gene fusion call. The *KMT2A* and *MLLT4* gene positions and orientations are indicated. Black dashed lines depict the breakpoint locations on each chromosome. (**C**) Chromosome 2 × Chromosome 13 Hi-C heatmap from specimen "ARMS C3". Genomic coordinates, gene locations, and sequencing coverage from Chromosome 2 and 13 are shown along the edges of the X and Y axes of the heatmap, respectively. Small black boxes overlaid on the heatmap are the Arima-SV pipeline genomic rearrangement calls. (**D**) Same as panel (**C**), except zoomed-in to the locus around the *PAX3::FOXO1* gene fusion call. The *PAX3* and *FOXO1* gene positions and orientations are indicated. Black dashed lines depict the breakpoint locations on each chromosome. In all Hi-C heatmaps, pairs of loci with more Hi-C read support appear as darker red entries in the Hi-C heatmap, pairs of loci with less Hi-C read support appear as lighter red entries, and pairs of loci with no Hi-C support appear white/gray entries.

While these concordance analyses were all carried out at a standardized sequencing depth of 50 million raw read-pairs, we also explored the minimum sequencing depths at which the clinically relevant gene fusions could be detected. In the FFPE sarcoma samples, 4/5 (80%) gene fusions could be detected at 25 million and 12.5 million raw read-pairs, and 3/5 (60%) at 5 million raw read-pairs (Supplemental Table S3). As all 5 FFPE sarcoma samples had an estimated 80–90% tumor cell content (Supplemental Tables S1 and S3), it is more likely that other factors, such as copy number and Hi-C data quality, affected

the minimum sequencing depth at which gene fusions could be detected. Furthermore, in the AML specimens, 4/5 (80%) gene fusions could be detected at 25 and 12.5 million raw read-pairs and 2/5 (40%) at 5 million raw read-pairs (Supplemental Table S3). There did not appear to be a correlation between the minimum sequencing depth at which gene fusions could be detected and the percentage of cells positive for the known rearrangement (Supplemental Table S3), albeit with a relatively small sample size. However, the one AML specimen insensitive at 25 million and 12.5 million raw reads was the only specimen amongst the fusion-positive AML concordance cases prepared as a non-viable frozen pellet, which had lower Hi-C data quality metrics (Supplemental Table S2), again indicating an interplay between Hi-C data quality profiles and analytical sensitivity that requires further systematic analysis. Unsurprisingly, no fusions were detected across all sequencing depths in the two fusion-negative AML specimens in the concordance cohort.

3.3. Driver-Negative Leukemias–Discovery Cohort

We then assessed a discovery cohort of leukemia specimens for which previous diagnostic testing had not identified any driver (i.e., genetic subtype defining) genomic rearrangements. Samples included one AML, eight B-ALL, and two T-ALL specimens (Tables 2 and S1). Similar to the concordance cases, we analyzed the data at a standardized depth of 50 million raw read-pairs. We detected clinically significant fusions in 3 of 11 cases (two *ZNF384::EP300* fusions and one *KMT2A::MLLT10* fusion), as well as potentially significant fusions in 2 of 11 cases (one *SKAP2::CDK6* fusion and one *ABHD17B::PTK2B* fusion) (Table 2). For example, in the "AML D1" case, Hi-C analysis detected a *KMT2A::MLLT10* gene fusion (Figure 3A,B), while previous clinical testing comprising of karyotyping, FISH, short-read NGS, and microarray did not detect this clinically significant rearrangement. This observation is consistent with reports of this rearrangement sometimes being cryptic and not visible on karyotype analysis, FISH, or microarray [40]. Indeed, an interpretation of the Hi-C signal pattern at the *KMT2A::MLLT10* breakpoint (Figure 3B) indicates an inversion of the 5′ portion of *KMT2A* and fusion to the 3′ portion of *MLLT10*, resulting in the expected *KMT2A::MLLT10* fusion gene orientation. Identification of the *KMT2A::MLLT10* gene fusion carries strong clinical significance; had it been detected in the prospective setting, it would have changed the pathology diagnosis, risk classification, and treatment approach [41]. *KMT2A::MLLT10* is considered a high-risk fusion in pediatric AML and is an indication for hematopoietic stem cell transplant in first remission [42,43]. There is also evidence that the addition of Gemtuzumab to conventional chemotherapy improves clinical outcomes for patients with *KMT2A*-rearranged AML [42]. In two other B-ALL cases ("B-ALL D8" and "B-ALL D6"), Hi-C analysis detected *ZNF384::EP300* gene fusions (Figure 3C–F), which previous clinical testing comprising of karyotyping, FISH, short-read NGS, and microarray did not detect (Table 2). This finding also carries clinical significance, whereby, had the *ZNF384::EP300* gene fusions been detected in the prospective setting, it would have changed the pathology diagnosis [41] and been associated with an intermediate prognosis. In addition, patients with *ZNF384* fusions to *EP300* have been reported to have lower relapse rates than patients with other *ZNF384* fusions [44]. Of note, this rearrangement is known to be cytogenetically cryptic, was not specifically tested for by FISH, and is balanced, so it was not detected by CMA. Furthermore, RNA-based fusion panel testing was performed at a reference laboratory for case B-ALL D8 but was negative, consistent with the panel not targeting *EP300* or *ZNF384*. This scenario underscores the utility of Hi-C, given its unbiased genome-wide nature for fusion detection with relatively low-pass coverage (~50 million raw read-pairs).

Similar to the analyses in the concordance cohort, we also determined the minimum sequencing depths at which the clinically relevant gene fusions could be detected. Across the five leukemia specimens with a clinically relevant gene fusion detected, 5/5 (100%) gene fusions could be detected at 25 and 12.5 million raw read-pairs and 3/5 (60%) at 5 million raw read-pairs (Supplemental Table S3).

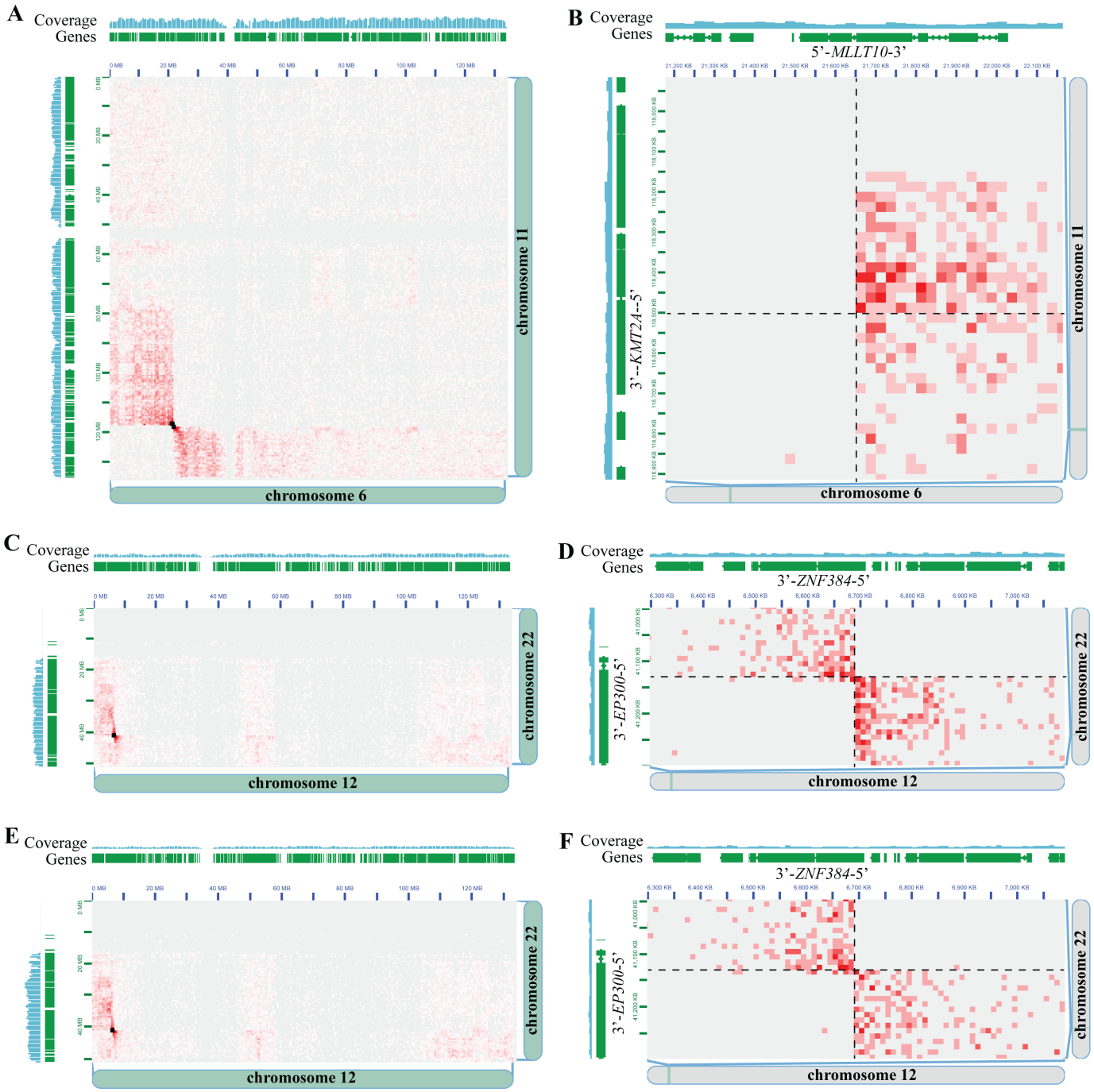

Figure 3. Hi-C detects clinically significant gene fusions not previously detected by clinical cytogenetic and molecular testing. (**A**) Chromosome 6 × Chromosome 11 Hi-C heatmap from specimen "AML D1". Genomic coordinates, gene locations, and sequencing coverage from Chromosome 6 and 11 are shown along the edges of the X and Y axes of the heatmap, respectively. Small black boxes overlaid on the heatmap are the Arima-SV pipeline genomic rearrangement calls. (**B**) Same as panel (**A**), except zoomed-in to the locus around the *KMT2A::MLLT10* gene fusion call. The *KMT2A* and *MLLT10* gene positions and orientations are indicated. Black dashed lines depict the breakpoint locations on each chromosome. (**C**) Chromosome 12 × Chromosome 22 Hi-C heatmap from specimen "B-ALL D8". Genomic coordinates, gene locations, and sequencing coverage from Chromosome 12 and 22 are shown along the edges of the X and Y axes of the heatmap, respectively. Small black boxes overlaid

on the heatmap are the Arima-SV pipeline genomic rearrangement calls. (**D**) Same as panel (**C**), except zoomed-in to the locus around the *ZNF384::EP300* gene fusion call. The *ZNF384* and *EP300* gene positions and orientations are indicated. Black dashed lines depict the breakpoint locations on each chromosome. (**E**) Same as panel (**C**), except from specimen "B-ALL D6". (**F**) Same as panel (**D**), except from specimen "B-ALL D6". In all Hi-C heatmaps, pairs of loci with more Hi-C read support appear as darker red entries in the Hi-C heatmap, pairs of loci with less Hi-C read support appear as lighter red entries, and pairs of loci with no Hi-C support appear white/gray entries.

Table 2. Hi-C detects clinically significant gene fusions not detected by prior clinical cytogenetic and molecular testing.

Sample ID	Cancer Type	Sample Source	Preservation (If Any)	Prior Dx Test Result	Hi-C Test Result	Clinical Impact
AML D1	AML	PBMCs	90% FBS/10% DMSO	Negative	*KMT2A::MLLT10*	Dx, Px, Tx
T-ALL D1	T-ALL	Bone Marrow	90% FBS/10% DMSO	Negative	*SKAP2::CDK6*	Tx *
T-ALL D2	T-ALL	Bone Marrow	None	Negative	Negative	N/A
B-ALL D1	B-ALL	Bone Marrow	None	Negative	Negative	N/A
B-ALL D2	B-ALL	Bone Marrow	None	Negative	Negative	N/A
B-ALL D3	B-ALL	Bone Marrow	90% FBS/10% DMSO	Negative	Negative	N/A
B-ALL D4	B-ALL	Bone Marrow	90% FBS/10% DMSO	Negative	Negative	N/A
B-ALL D5	B-ALL	PBMCs	90% FBS/10% DMSO	Negative	Negative	N/A
B-ALL D6	B-ALL	Bone Marrow	90% FBS/10% DMSO	Negative	*ZNF384::EP300*	Dx, Px
B-ALL D7	B-ALL	Bone Marrow	90% FBS/10% DMSO	Negative	*ABHD17B::PTK2B*	Dx, Px **
B-ALL D8	B-ALL	Bone Marrow	90% FBS/10% DMSO	Negative	*ZNF384-EP300*	Dx, Px

AML = Acute Myeloid Leukemia; ALL = Acute Lymphoblastic Leukemia; PBMC = Peripheral Blood Mononuclear Cell; FBS = Fetal Bovine Serum; DMSO = Dimethyl Sulfoxide; Dx = Diagnostic Clinical Impact; Px = Prognostic Clinical Impact; Tx = Therapeutic Clinical Impact; Clinical Impact is determined according to WHO and NCCN guidelines. * Phase I clinical trials for CDK4/6 inhibitors have been completed in pediatric and young adults with ALL [45]. ** PTK2Br is diagnostic and prognostic according to NCCN guidelines for ALL [46].

4. Discussion

We conducted an institutional proof of concept evaluation of Arima Genomics' Hi-C technology for the unbiased genome-wide detection of clinically relevant genomic rearrangements in a retrospective cohort of pediatric solid tumors and hematologic cancers. Using a standardized sequencing coverage of 50 million raw Hi-C read-pairs per sample (approximately 5X raw genomic coverage), we observed 100% (12/12) concordance between Hi-C and prior clinical genetic testing for clinically relevant gene fusions. Additionally, in pediatric leukemias without any previously detected genomic rearrangements via available clinical cytogenetic and molecular testing, Hi-C detected a clinically relevant gene fusion in ~45% (5/11) of cases—providing diagnostically, prognostically, and therapeutically significant information.

One notable result from this study is that Hi-C is robust to a variety of clinical specimen types and preservation methods —it is routinely obtained and processed in hematologic and solid tumor clinical and research laboratory testing workflows—and to various specimen preservation methods and archival periods. Importantly, for solid tumor clinical testing, Hi-C performed well using FFPE tissue, which represents a unique and powerful benefit to Hi-C technology compared to emerging long-read or optical mapping technologies whose advantages are dependent on the analysis of high-molecular-weight DNA, which is difficult to obtain from FFPE specimens. Furthermore, the FFPE specimens analyzed in this study had archival periods of 9 to 13 years. This suggests that in addition to prospective solid tumor testing, Hi-C technology opens up a range of research opportunities for pathologists or other clinical research investigators to study genomic rearrangements in archived FFPE tissue material. This is particularly important given that RNA-seq may perform poorly when analyzing FFPE specimens following prolonged storage due to RNA degradation [16,17]. In the hematological cancer setting, Hi-C detected clinically relevant genomic rearrangements in both viably and non-viably preserved specimens, although the data were of significantly better quality in viably preserved specimens. More systematic studies may be needed to tease apart the relationship between preservation method, Hi-C

data quality, and fusion detection performance. Along those lines, this study also raises the need to define the compatibility of Hi-C in other sample types or preservation contexts that arise in clinical testing workflows for hematologic cancers. For example, compatibility with blood collected in blood collection tubes other than the ones used in this study (EDTA), blood processed after various time intervals between collection and Hi-C sample preparation (blood stability), and compatibility with other fixatives used in clinical testing workflows (e.g., acetic acid and methanol).

The genome-wide, partner-agnostic nature of the Hi-C approach utilized in this study has notable benefits for clinical testing compared to other clinical testing methods. For example, FISH requires the selection of probes for the assay and, depending on the FISH probe design, is potentially unable to resolve the fusion partner. FISH is also often performed serially as a single-gene test [47]. In contrast, the genome-wide implementation of Hi-C can detect rearrangements involving any gene across the whole genome simultaneously and detect both partners for all rearrangements identified. However, FISH is inherently a technology with single-cell resolution and is, therefore, capable of detecting fusions even when the percentage of tumor cells is very low, whereas the limit of detection for Hi-C remains to be defined.

Targeted RNA-seq has similar limitations since it is restricted to the list of genes on a given panel but can be multiplexed to hundreds of genes and can be partner-agnostic (e.g., AMP), assuming RNA quality and/or workflow complexity do not preclude RNA-seq analysis. While targeted RNA-seq can detect fusions involving genes already known (or suspected to be) of clinical relevance based on the probe/primer design, the genome-wide nature of Hi-C allows it to detect gene fusions of both known and unknown relevance, potentiating the discovery of novel biomarkers, disease mechanisms, or therapeutic targets to advance clinical research. Furthermore, RNA-seq only detects gene fusions when a fusion transcript is produced and expressed at detectable levels. It is, therefore, insensitive to other types of genomic rearrangements, which do not produce a fusion transcript, such as promoter swaps or enhancer hijacking events. In contrast, the genome-wide and DNA-based nature of Hi-C allows it to detect these types of genomic rearrangements, as exemplified in a recent case study where Arima Genomics' Hi-C detected an *IGH::IRF4* rearrangement in a lymphoma specimen. This rearrangement was previously undetected by prior RNA-seq (and FISH) analyses despite both assays using probes targeting *IRF4* (REF) [30]. While promising, further studies focused on detecting promoter swap or enhancer hijacking rearrangements using Hi-C would be valuable. Finally, relative to FISH and RNA-seq, the DNA-based and genome-wide nature of Hi-C gives it the potential to detect a fuller spectrum of genomic variation from a single test, including CNVs and sequence variants, as the technology matures and expands.

While this institutional proof of concept evaluation of Arima Genomics' Hi-C technology for genomic rearrangement testing was successful, additional clinical validation studies, such as tumor-normal dilution studies to define the limit of detection (LOD) more rigorously, would be needed to implement Hi-C into clinical laboratory workflows for either solid or hematological cancer testing. While these efforts lie ahead for most clinical laboratories, Arima Genomics' Hi-C technology is already available in the commercial clinical laboratory setting for genomic rearrangement analysis services (Aventa Genomics (Orlando, FL, USA)).

5. Conclusions

Arima Genomics' Hi-C technology was concordant with standard clinical diagnostic testing methods in solid and hematologic pediatric cancer specimens. Furthermore, the study demonstrated how Hi-C sequencing could provide additional diagnostic, prognostic, and therapeutic value by identifying clinically significant genomic rearrangements potentially missed by current clinical diagnostic testing workflows.

Supplementary Materials: The following supporting information can be downloaded at https://www.mdpi.com/article/10.3390/cancers16172936/s1, Figure S1: Hi-C analysis determines the rearrangement type from formalin-fixed paraffin-embedded solid tumors and is concordant with karyotype analysis. Table S1: Pediatric sarcoma and leukemia specimen characteristics; Table S2: Hi-C data quality metrics; Table S3: Hi-C sub-sampling sensitivity analysis.

Author Contributions: Conceptualization, A.D.S. and M.S.F.; Data curation, A.D.S., A.A.A., L.A.L. and M.S.F.; Formal analysis, K.S.; Funding acquisition, A.D.S.; Methodology, K.S., S.M., D.R. and L.V.M.; Project administration, M.S.F.; Resources, A.A.A. and M.S.F.; Supervision, A.D.S. and M.S.F.; Visualization, A.D.S.; Writing–original draft, A.D.S. and M.S.F.; Writing–review and editing, A.D.S., A.A.A., E.M.G., L.A.L., T.P., I.P., B.Y. and M.S.F. All authors have read and agreed to the published version of the manuscript.

Funding: Arima Genomics received support from NIH NCI grant # R44CA247185. E.G. reports grants from the Alex Lemonade Stand Foundation, Braden's Hope for Childhood Cancer, Noah's Bandage Project, Children's Cancer Research Fund, and the American Cancer Society. T.P. reports grants from the Helmsley Foundation and NIH (R44HG011897, 1UC4DK117483-01, 5UL1TR002366-04). M.S.F. reports grants from Braden's Hope for Childhood Cancer, Big Slick, the Black & Veatch Foundation, Masonic Cancer Alliance, Noah's Bandage Project, Elizabeth and Monte McDowell, Cancer Center Auxiliary, and the Department of Defense (W81XWH-20-1-0358).

Institutional Review Board Statement: The study was conducted according to the guidelines of the Declaration of Helsinki and approved by the Institutional Review Board of Children's Mercy Hospital (CMH, Kansas City, MO, USA) (initial protocol Study00000718 approved on 24 September 2021, Study00000085 approved on 15 June 2018, and Study15030100 approved on 21 March 2016).

Informed Consent Statement: Informed consent was obtained from all subjects with leukemia involved in the study. Patient consent was waived for the individuals with rhabdomyosarcoma due to these being historic samples (stored for $\geq$9 years), with the vast majority of patients deceased and these samples being de-identified (non-human subjects).

Data Availability Statement: The (non-identifying) data presented in this study are available, on request, from the corresponding author due to privacy restrictions.

Acknowledgments: Medical writing and editing services were provided by Maartje Wouters, which was funded by Arima Genomics. The authors would like to thank the patients and families who donated their samples for this research. The authors would also like to thank Lucia Laude and the Histology Core. Tumor bank study personnel: Judy Vun, Amie Hatfield, and Robin Ryan, as well as Jason Seymour and Keiondra Sanders in the Children's Mercy Research Institute Biorepository for their assistance with sample collection and processing. Finally, M.S.F. would like to thank the Children's Mercy Research Institute, Braden's Hope for Childhood Cancer, Big Slick, Elizabeth and Monte McDowell, the Masonic Cancer Alliance, the Cancer Center Auxiliary, and the Black & Veatch Foundation for their generous support.

Conflicts of Interest: A.D.S., K.S. and S.M. are current employees of Arima Genomics at the time of manuscript preparation. D.R. and L.V.M. are former employees of Arima Genomics. E.G. reports consulting fees from Jazz Pharmaceuticals, Syndax Pharmaceuticals; and honoraria from Jazz Pharmaceuticals, Speakers Bureau; stock or stock options from Moderna. T.P. reports consulting fees from Hitachi High Tech America; honoraria from the University of Nebraska, University of Toronto, TD Cowen; travel support from the University of Nebraska, University of Toronto, TD Cowen, Hitachi HTA, University of Washington, Pacific Biosciences. A.A.A., L.A.L., I.P. and B.Y. report no conflict of interest. M.S.F. reports honoraria from the Bayer Speakers Bureau and PacBio Speakers Bureau.

References

1. Siegel, R.L.; Miller, K.D.; Fuchs, H.E.; Jemal, A. Cancer statistics, 2022. *CA Cancer J. Clin.* **2022**, *72*, 7–33. [CrossRef]
2. Ahmed, A.A.; Vundamati, D.S.; Farooqi, M.S.; Guest, E. Precision Medicine in Pediatric Cancer: Current Applications and Future Prospects. *High. Throughput* **2018**, *7*, 39. [CrossRef]
3. PDQ® Pediatric Treatment Editorial Board. Childhood Cancer Genomics (PDQ(R)): Health Professional Version. Available online: https://www.cancer.gov/types/childhood-cancers/pediatric-genomics-hp-pdq (accessed on 7 February 2024).

4. Grobner, S.N.; Worst, B.C.; Weischenfeldt, J.; Buchhalter, I.; Kleinheinz, K.; Rudneva, V.A.; Johann, P.D.; Balasubramanian, G.P.; Segura-Wang, M.; Brabetz, S.; et al. The landscape of genomic alterations across childhood cancers. *Nature* **2018**, *555*, 321–327. [CrossRef] [PubMed]
5. Ma, X.; Liu, Y.; Liu, Y.; Alexandrov, L.B.; Edmonson, M.N.; Gawad, C.; Zhou, X.; Li, Y.; Rusch, M.C.; Easton, J.; et al. Pan-cancer genome and transcriptome analyses of 1,699 paediatric leukaemias and solid tumours. *Nature* **2018**, *555*, 371–376. [CrossRef] [PubMed]
6. Rahal, Z.; Abdulhai, F.; Kadara, H.; Saab, R. Genomics of adult and pediatric solid tumors. *Am. J. Cancer Res.* **2018**, *8*, 1356–1386. [PubMed]
7. Smith, S.C.; Warren, L.M.; Cooley, L.D. Maintaining a methods database to optimize solid tumor tissue culture: Review of a 15-year database from a single institution. *Cancer Genet.* **2019**, *233–234*, 96–101. [CrossRef]
8. Simons, A.; Sikkema-Raddatz, B.; de Leeuw, N.; Konrad, N.C.; Hastings, R.J.; Schoumans, J. Genome-wide arrays in routine diagnostics of hematological malignancies. *Hum. Mutat.* **2012**, *33*, 941–948. [CrossRef]
9. Rieder, H.; Sommerlad, C.; Mehraein, Y.; Giersberg, M.; Marben, K.; Rehder, H. Formalin-Fixed and Paraffin-Embedded Tissue Sections. In *FISH Technology*; Rautenstrauss, B.W., Liehr, T., Eds.; Springer: Berlin/Heidelberg, Germany, 2002; pp. 148–161.
10. Peterson, J.F.; Aggarwal, N.; Smith, C.A.; Gollin, S.M.; Surti, U.; Rajkovic, A.; Swerdlow, S.H.; Yatsenko, S.A. Integration of microarray analysis into the clinical diagnosis of hematological malignancies: How much can we improve cytogenetic testing? *Oncotarget* **2015**, *6*, 18845–18862. [CrossRef]
11. Akkari, Y.; Dobin, S.; Best, R.G.; Leung, M.L. Exploring current challenges in the technologist workforce of clinical genomics laboratories. *Genet. Med. Open* **2023**, *1*, 100806. [CrossRef]
12. Engvall, M.; Cahill, N.; Jonsson, B.I.; Hoglund, M.; Hallbook, H.; Cavelier, L. Detection of leukemia gene fusions by targeted RNA-sequencing in routine diagnostics. *BMC Med. Genom.* **2020**, *13*, 106. [CrossRef]
13. Avenarius, M.R.; Miller, C.R.; Arnold, M.A.; Koo, S.; Roberts, R.; Hobby, M.; Grossman, T.; Moyer, Y.; Wilson, R.K.; Mardis, E.R.; et al. Genetic Characterization of Pediatric Sarcomas by Targeted RNA Sequencing. *J. Mol. Diagn.* **2020**, *22*, 1238–1245. [CrossRef]
14. Chebib, I.; Taylor, M.S.; Nardi, V.; Rivera, M.N.; Lennerz, J.K.; Cote, G.M.; Choy, E.; Lozano Calderon, S.A.; Raskin, K.A.; Schwab, J.H.; et al. Clinical Utility of Anchored Multiplex Solid Fusion Assay for Diagnosis of Bone and Soft Tissue Tumors. *Am. J. Surg. Pathol.* **2021**, *45*, 1127–1137. [CrossRef]
15. Zheng, Z.; Liebers, M.; Zhelyazkova, B.; Cao, Y.; Panditi, D.; Lynch, K.D.; Chen, J.; Robinson, H.E.; Shim, H.S.; Chmielecki, J.; et al. Anchored multiplex PCR for targeted next-generation sequencing. *Nat. Med.* **2014**, *20*, 1479–1484. [CrossRef]
16. Cronin, M.; Pho, M.; Dutta, D.; Stephans, J.C.; Shak, S.; Kiefer, M.C.; Esteban, J.M.; Baker, J.B. Measurement of gene expression in archival paraffin-embedded tissues: Development and performance of a 92-gene reverse transcriptase-polymerase chain reaction assay. *Am. J. Pathol.* **2004**, *164*, 35–42. [CrossRef]
17. Penland, S.K.; Keku, T.O.; Torrice, C.; He, X.; Krishnamurthy, J.; Hoadley, K.A.; Woosley, J.T.; Thomas, N.E.; Perou, C.M.; Sandler, R.S.; et al. RNA expression analysis of formalin-fixed paraffin-embedded tumors. *Lab. Investig.* **2007**, *87*, 383–391. [CrossRef] [PubMed]
18. Brown, P.; Inaba, H.; Annesley, C.; Beck, J.; Colace, S.; Dallas, M.; DeSantes, K.; Kelly, K.; Kitko, C.; Lacayo, N.; et al. Pediatric Acute Lymphoblastic Leukemia, Version 2.2020, NCCN Clinical Practice Guidelines in Oncology. *J. Natl. Compr. Cancer Netw.* **2020**, *18*, 81–112. [CrossRef] [PubMed]
19. Smith, A.C.; Neveling, K.; Kanagal-Shamanna, R. Optical genome mapping for structural variation analysis in hematologic malignancies. *Am. J. Hematol.* **2022**, *97*, 975–982. [CrossRef]
20. Dixon, J.R.; Xu, J.; Dileep, V.; Zhan, Y.; Song, F.; Le, V.T.; Yardimci, G.G.; Chakraborty, A.; Bann, D.V.; Wang, Y.; et al. Integrative detection and analysis of structural variation in cancer genomes. *Nat. Genet.* **2018**, *50*, 1388–1398. [CrossRef] [PubMed]
21. Harewood, L.; Kishore, K.; Eldridge, M.D.; Wingett, S.; Pearson, D.; Schoenfelder, S.; Collins, V.P.; Fraser, P. Hi-C as a tool for precise detection and characterisation of chromosomal rearrangements and copy number variation in human tumours. *Genome Biol.* **2017**, *18*, 125. [CrossRef]
22. Iyyanki, T.; Zhang, B.; Wang, Q.; Hou, Y.; Jin, Q.; Xu, J.; Yang, H.; Liu, T.; Wang, X.; Song, F.; et al. Subtype-associated epigenomic landscape and 3D genome structure in bladder cancer. *Genome Biol.* **2021**, *22*, 105. [CrossRef]
23. Jacobson, E.C.; Grand, R.S.; Perry, J.K.; Vickers, M.H.; Olins, A.L.; Olins, D.E.; O'Sullivan, J.M. Hi-C detects novel structural variants in HL-60 and HL-60/S4 cell lines. *Genomics* **2020**, *112*, 151–162. [CrossRef]
24. Mallard, C.; Johnston, M.J.; Bobyn, A.; Nikolic, A.; Argiropoulos, B.; Chan, J.A.; Guilcher, G.M.T.; Gallo, M. Hi-C detects genomic structural variants in peripheral blood of pediatric leukemia patients. *Cold Spring Harb. Mol. Case Stud.* **2022**, *8*, a006157. [CrossRef] [PubMed]
25. Mathur, R.; Wang, Q.; Schupp, P.G.; Nikolic, A.; Hilz, S.; Hong, C.; Grishanina, N.R.; Kwok, D.; Stevers, N.O.; Jin, Q.; et al. Glioblastoma evolution and heterogeneity from a 3D whole-tumor perspective. *Cell* **2024**, *187*, 446–463.e16. [CrossRef] [PubMed]
26. Wang, J.; Huang, T.Y.; Hou, Y.; Bartom, E.; Lu, X.; Shilatifard, A.; Yue, F.; Saratsis, A. Epigenomic landscape and 3D genome structure in pediatric high-grade glioma. *Sci. Adv.* **2021**, *7*, eabg4126. [CrossRef] [PubMed]
27. Wang, X.; Luan, Y.; Yue, F. EagleC: A deep-learning framework for detecting a full range of structural variations from bulk and single-cell contact maps. *Sci. Adv.* **2022**, *8*, eabn9215. [CrossRef]
28. Xu, J.; Song, F.; Lyu, H.; Kobayashi, M.; Zhang, B.; Zhao, Z.; Hou, Y.; Wang, X.; Luan, Y.; Jia, B.; et al. Subtype-specific 3D genome alteration in acute myeloid leukaemia. *Nature* **2022**, *611*, 387–398. [CrossRef] [PubMed]

29. Xu, Z.; Lee, D.S.; Chandran, S.; Le, V.T.; Bump, R.; Yasis, J.; Dallarda, S.; Marcotte, S.; Clock, B.; Haghani, N.; et al. Structural variants drive context-dependent oncogene activation in cancer. *Nature* **2022**, *612*, 564–572. [CrossRef]
30. Prior, D.; Schmitt, A.D.; Louissaint, A.; Mata, D.A.; Massaro, S.; Nardi, V.; Xu, M.L. Large B-cell lymphoma with mystery rearrangement: Applying Hi-C to the detection of clinically relevant structural abnormalities. *Br. J. Haematol.* **2024**. [CrossRef]
31. Arima SV Pipeline for Mapping, SV Detection and QC. GitHub Repository 2023. Available online: https://github.com/ArimaGenomics/Arima-SV-Pipeline (accessed on 10 July 2024).
32. Wingett, S.; Ewels, P.; Furlan-Magaril, M.; Nagano, T.; Schoenfelder, S.; Fraser, P.; Andrews, S. HiCUP: Pipeline for mapping and processing Hi-C data. *F1000Research* **2015**, *4*, 1310. [CrossRef]
33. Durand, N.C.; Shamim, M.S.; Machol, I.; Rao, S.S.; Huntley, M.H.; Lander, E.S.; Aiden, E.L. Juicer Provides a One-Click System for Analyzing Loop-Resolution Hi-C Experiments. *Cell Syst.* **2016**, *3*, 95–98. [CrossRef]
34. Durand, N.C.; Robinson, J.T.; Shamim, M.S.; Machol, I.; Mesirov, J.P.; Lander, E.S.; Aiden, E.L. Juicebox Provides a Visualization System for Hi-C Contact Maps with Unlimited Zoom. *Cell Syst.* **2016**, *3*, 99–101. [CrossRef]
35. Hayes, M.; Nguyen, A.; Islam, R.; Butler, C.; Tran, E.; Mullins, D.; Hicks, C. HolistIC: Leveraging Hi-C and whole genome shotgun sequencing for double minute chromosome discovery. *Bioinformatics* **2022**, *38*, 1208–1215. [CrossRef] [PubMed]
36. Chapman, O.S.; Luebeck, J.; Sridhar, S.; Wong, I.T.; Dixit, D.; Wang, S.; Prasad, G.; Rajkumar, U.; Pagadala, M.S.; Larson, J.D.; et al. Circular extrachromosomal DNA promotes tumor heterogeneity in high-risk medulloblastoma. *Nat. Genet.* **2023**, *55*, 2189–2199. [CrossRef] [PubMed]
37. Zhu, Y.; Gujar, A.D.; Wong, C.H.; Tjong, H.; Ngan, C.Y.; Gong, L.; Chen, Y.A.; Kim, H.; Liu, J.; Li, M.; et al. Oncogenic extrachromosomal DNA functions as mobile enhancers to globally amplify chromosomal transcription. *Cancer Cell* **2021**, *39*, 694–707.e7. [CrossRef] [PubMed]
38. Helmsauer, K.; Valieva, M.E.; Ali, S.; Chamorro Gonzalez, R.; Schopflin, R.; Roefzaad, C.; Bei, Y.; Dorado Garcia, H.; Rodriguez-Fos, E.; Puiggros, M.; et al. Enhancer hijacking determines extrachromosomal circular MYCN amplicon architecture in neuroblastoma. *Nat. Commun.* **2020**, *11*, 5823. [CrossRef] [PubMed]
39. Wu, S.; Turner, K.M.; Nguyen, N.; Raviram, R.; Erb, M.; Santini, J.; Luebeck, J.; Rajkumar, U.; Diao, Y.; Li, B.; et al. Circular ecDNA promotes accessible chromatin and high oncogene expression. *Nature* **2019**, *575*, 699–703. [CrossRef]
40. Peterson, J.F.; Sukov, W.R.; Pitel, B.A.; Smoley, S.A.; Pearce, K.E.; Meyer, R.G.; Williamson, C.M.; Smadbeck, J.B.; Vasmatzis, G.; Hoppman, N.L.; et al. Acute leukemias harboring KMT2A/MLLT10 fusion: A 10-year experience from a single genomics laboratory. *Genes. Chromosomes Cancer* **2019**, *58*, 567–577. [CrossRef]
41. WHO Classification of Tumours Editorial Board. Paediatric Tumours. In *WHO Classification of Tumours*, 5th ed.; World Health Organization: Geneva, Switzerland, 2023; Volume 7.
42. Pollard, J.A.; Guest, E.; Alonzo, T.A.; Gerbing, R.B.; Loken, M.R.; Brodersen, L.E.; Kolb, E.A.; Aplenc, R.; Meshinchi, S.; Raimondi, S.C.; et al. Gemtuzumab Ozogamicin Improves Event-Free Survival and Reduces Relapse in Pediatric KMT2A-Rearranged AML: Results from the Phase III Children's Oncology Group Trial AAML0531. *J. Clin. Oncol.* **2021**, *39*, 3149–3160. [CrossRef]
43. van Weelderen, R.E.; Klein, K.; Harrison, C.J.; Jiang, Y.; Abrahamsson, J.; Arad-Cohen, N.; Bart-Delabesse, E.; Buldini, B.; De Moerloose, B.; Dworzak, M.N.; et al. Measurable Residual Disease and Fusion Partner Independently Predict Survival and Relapse Risk in Childhood KMT2A-Rearranged Acute Myeloid Leukemia: A Study by the International Berlin-Frankfurt-Munster Study Group. *J. Clin. Oncol.* **2023**, *41*, 2963–2974. [CrossRef]
44. Hirabayashi, S.; Butler, E.R.; Ohki, K.; Kiyokawa, N.; Bergmann, A.K.; Moricke, A.; Boer, J.M.; Cave, H.; Cazzaniga, G.; Yeoh, A.E.J.; et al. Clinical characteristics and outcomes of B-ALL with ZNF384 rearrangements: A retrospective analysis by the Ponte di Legno Childhood ALL Working Group. *Leukemia* **2021**, *35*, 3272–3277. [CrossRef]
45. Raetz, E.A.; Teachey, D.T.; Minard, C.; Liu, X.; Norris, R.E.; Denic, K.Z.; Reid, J.; Evensen, N.A.; Gore, L.; Fox, E.; et al. Palbociclib in combination with chemotherapy in pediatric and young adult patients with relapsed/refractory acute lymphoblastic leukemia and lymphoma: A Children's Oncology Group study (AINV18P1). *Pediatr. Blood Cancer* **2023**, *70*, e30609. [CrossRef] [PubMed]
46. Shah, B.; Mattison, R.J.; Abboud, R.; Abdelmessieh, P.; Patricia Aoun, P.; Burke, P.W.; DeAngelo, D.J.; Lurie, R.H.; Fathi, A.T.; Gauthier, J.; et al. Acute Lymphoblastic Leukemia, Version 4.2023, NCCN Clinical Practice Guidelines in Oncology. *J. Natl. Compr. Cancer Netw.* **2024**. Available online: https://www.nccn.org/guidelines/guidelines-detail (accessed on 11 July 2024).
47. Quessada, J.; Cuccuini, W.; Saultier, P.; Loosveld, M.; Harrison, C.J.; Lafage-Pochitaloff, M. Cytogenetics of Pediatric Acute Myeloid Leukemia: A Review of the Current Knowledge. *Genes* **2021**, *12*, 924. [CrossRef] [PubMed]